COBEM 2023 27TH INTERNATIONAL CONGRESS OF MECHANICAL ENGENEERING

ABCM Brazilian Society of Mechanical Sciences and Engineering
27th ABCM International Congress of Mechanical Engineering
December 04-08, 2023, Florianópolis-SC, Brazil

COB-2023-0943
Explainable AI applied to Malfanction Parameter Determination on Rotating Machines using Bayesian Neural Networks and Sobol Index

Olympio Belli
e-mail: o185244@dac.unicamp.br
Hélio Fiori de Castro
e-mails: hfc@unicamp.br
University of Campinas - Unicamp

Abstract. *Not rarely, rotating components perform critical functions in mechanical systems that require high levels of reliability. As an emerging line of research, fault detection in rotating machinery is increasingly being carried out using artificial intelligence (AI) techniques fed by data from vibration, temperature, and sound sensors. These types of algorithms have been relatively successful due to their ability to handle with a large set of input data and provide high accuracy in diagnostics. However, these techniques still lack explainability and are often referred as black boxes. To address this problem, this paper aims to combine the ability of Bayesian Neural Networks (BNNs) to express uncertainty with global sensitivity analysis using Sobol Index to determine which inputs are more determinant for the meta-models formulated. In this sense, BNNs were trained to regress malfunction parameters of a double rotor connected by a coupling. The regressed faults were: crack size, coupling misalignment angle, and distance. The AI models were trained using a data set generated by numerical simulations whose bearing displacement data were processed using the full spectrum transform. Finally, the first and second-order Sobol index analysis was applied and validated, identifying the most influential inputs for model prediction.*

Keywords: *Explainable Artificial Intelligence, Bayesian Neural Networks, Condition-Based Maintenance, Rotor Dynamics and Sobol Index*

1. INTRODUCTION

It is of great importance in mechanical systems to identify possible deviations from standard operation. In the rotating machinery branch, this issue is crucial due to its extensive use in various types of equipment. Not rarely, rotating components perform critical functions in mechanical systems that require high levels of reliability. These systems may be employed in environments and operating conditions that are vulnerable to failure due to fatigue, wear, corrosion, and assembly errors Friswell (2010).

In the field of fault parameter diagnosis, there are several works related to each type of failure. For the determination of unbalanced parameters, it is worth mentioning Xie *et al.* (2016), which regressed unbalance data on a helicopter rotor. In Zang *et al.* (2018) the unbalance rotor based on sparsity control of the residual model was estimated, and finally, the paper by Luu and Hai (2020) did a dynamic balancing system with a multiple regression model. The work of Srinivas *et al.* (2021) proposes a model for the determination of angular and parallel misalignment parameters. For shaft cracking, the work of Ellis *et al.* (2022) proposes a model to infer the crack size in turbine blades and thereby calculate the remaining life before failure.

As an emerging line of research in recent years, fault detection in rotating machinery is increasingly being carried out using artificial intelligence (AI) techniques fed by data from vibration, temperature, sound, and image sensors Jardine *et al.* (2006). These types of algorithms have been relatively successful due to their ability to handle a large set of input data, provide high accuracy in machine diagnostics, and continuous monitoring Russell (2016). However, these statistical techniques still lack explainability and are often referred to as black boxes Castelvecchi (2016). Furthermore, these types of models, with a few exceptions, do not possess extrapolation capabilities and do not provide early warning to the user when the model is extrapolating and when the model is interpolating predictions between training data Belli (2023). Nowadays there is a huge demand in society for explainable and interpretable models Rudin (2019), from applications touching the ethical field Goodman and Flaxman (2017) to reliability in engineering Oh *et al.* (2023).

To address this problem, this paper aims to combine the ability of Bayesian Neural Networks (BNNs) to express uncertainty Gal and Ghahramani (2015) with global sensitivity analysis using Sobol Index to determine which inputs are more determinant for the meta-models formulated Štrumbelj and Kononenko (2014). In this work, the approach to Bayesian inference used was by applying the Monte Carlo Dropout technique that was first described in Gal and Ghahramani (2015). This method has been employed in situations where higher diagnostic reliability is needed, such as

in the medical field Lee and Kim (2022) and Ju *et al.* (2022) and in critical engineering systems Bae *et al.* (2022) and Tong *et al.* (2022). The Sobol index has been used to explain nonlinear models AI in Pan *et al.* (2021), Wang *et al.* (2023), and Fel *et al.* (2021).

In this sense, BNNs were trained to regress malfunction parameters of a double rotor with a coupling. The regressed faults were: coupling misalignment angle and distance, and crack size. The AI models were trained using a data set generated by numerical simulations whose bearing displacement data were processed using the full spectrum transform. The input parameters of the finite element model were modeled with probabilistic distributions and sampled using Monte Carlo. After training, the models were evaluated in their uncertainty expression, verifying that the higher the uncertainty, the higher the error performed in the predictions. Finally, the first and second-order Sobol index analyses were applied and validated, identifying the most influential inputs for model prediction.

2. OBJECTIVES

This paper aims to investigate the possibility of applying the Sobol index analysis combined with uncertainty quantification in Bayesian neural network to address the explainability to the AI diagnosis model applied to malfunction parameter determination in rotor machines in situations of shaft crack, angular and parallel misalignment.

3. METHODOLOGY

3.1 Multi-Fault Rotor Model

The basic model for simulating and modeling rotating machines is composed of a rotor, bearings and supporting structures. Many other variations can be included in the model to better represent the physics of the problem. In these theoretical models there are parameter inputs that characterize the machine such as the mass, rotational speed, damping coefficient related to energy dissipation, and stiffness coefficient. This mathematical model is formulated for modeling application with the Finite Element Method (FEM). The modeling of the Multi-Fault Rotor will follow the paper Garoli *et al.* (2019).

The shaft elements are modeled with Timoshenko beams of circular section which makes it possible to include the phenomenon of shear and rotational inertia. The formulation used for determines the mass matrix, rotation inertia matrix, gyroscopic matrix and the stiffness matrix follow Lalanne and Ferraris (1998). The global equation is shown bellow in 1

$$\mathbf{M} \cdot \ddot{\mathbf{q}} + (\mathbf{C} + \Omega \cdot \mathbf{G}) \cdot \dot{\mathbf{q}} + \mathbf{K} \cdot \mathbf{q} = \mathbf{F} \tag{1}$$

Where the variables $\mathbf{M}$, $\mathbf{C}$, $\mathbf{G}$ and $\mathbf{K}$ are the global mass, damping, gyroscopic effect and stiffness matrices. The vector $\mathbf{F}$ is the forces that are applied to the model. The variable $\mathbf{q}$, Ω are the displacement and is the angular velocity of the rotor, respectively. The construction data used for the rotor simulation is shown in Table 1:

Table 1. Construtive Parameters of the Simulated Rotor

Construtive Parameters of the Simulated Rotor								
Model Parameters	**Value**	**Unit**	**Model Parameters**	**Value**	**Unit**	**Model Parameters**	**Value**	**Unit**
Shaft Lengths	631.5	[mm]	Bearings Diameters	31	[mm]	Shafts Diameters	12	[mm]
Lubricating Oli Viscosity	40	[mPa.s]	Inner Disk Diameter	12	[mm]	Inner Coupling Disks Diameter	4	[mm]
Outer Disks Diameters	90	[mm]	Numer of Coupling Bolts	4	unit.	Disk Thickness	45	[mm]
Shear Modulus (G)	79.6	[MPa]	Elasticity Modulus (G)	211	[GPa]	Density	7860	[kg/m³]

The diagram representing the physical aspects of the rotor is shown below in Figure 1:

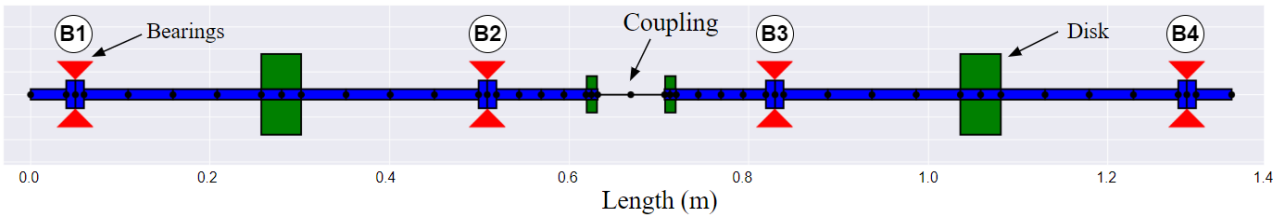

Figure 1. Rotor's Diagram.

3.2 Journal Bearing Modeling

The modeling of hydrodynamic bearings is realized by changing the stiffness and damping matrices of the elements that model them. In a simplified way, the Timoshenko beam elements in which the bearings are located have the behavior of their degrees of freedom altered by the inclusion of stiffness and damping coefficients that characterize the bearing. This proposition was made by Lund and Sternlicht (1962) for the modeling of hydrodynamic bearings. In purpose of simplifying the mathematical modeling, the short bearing assumption proposed by Ocvirk (1952) is assumed, in which it is possible to disregard the pressure variation in the bearing circumference direction and thus obtain an analytical solution by Reynolds.To include the effect of the short hydrodynamic bearing in the model just add the coefficients to the respective degrees of freedom in the finite element. The mathematical approach to this proposition is found in Krämer (1993). Finally, the foundation is considered to be infinitely rigid and for this reason has no influence on this model.

3.3 Model for Faults Simulation

Unbalance is one of the most common faults in rotating machines, since some level of unbalance is always found. No matter how perfectly a machine is manufactured, some assembly deviation always occurs. (adapted from Friswell (2010)) The presence of unbalance in the rotor generates a radial force causing an increase in the oscillatory motion of the rotor increasing the possibility of machine degradation for this reason. (adapted from Mohanty (1989)) For its correction it is usually balanced the rotor. Besides causing vibrations at the synchronous frequency (1X) Hatch (2002). The unbalancing force matrix was add to the model as described according to Lalanne and Ferraris (1998). In the equation 2 is shown the formulation of the unbalance force.

$$\begin{bmatrix} 0 \\ \vdots \\ F_u \\ F_w \\ 0 \\ \vdots \\ 0 \end{bmatrix} = \begin{bmatrix} 0 & 0 \\ \vdots & \vdots \\ m_u d\Omega^2 & 0 \\ 0 & m_u d\Omega^2 \\ 0 & 0 \\ \vdots & \vdots \\ 0 & 0 \end{bmatrix} \cdot \begin{bmatrix} \sin(\Omega t + \beta) \\ \cos(\Omega t + \beta) \end{bmatrix} \tag{2}$$

In the equation, m_u, d and β are respectively the unbalance mass, the mass eccentricity, and as the unbalance phase angle.

Misalignment can be characterized as an angular or parallel deviation with respect to the coaxial shaft of a coupling connecting two rotors. In the presence of this shaft irregularity in the machine connection preload forces are introduced into the coupling which are then transmitted to the different components of the machine reducing its useful life. (adapted from Piotrowski (1952)) In the work of Dewell and Mitchell (1984), a spectral analysis was used for the determination of misalignment in flexible couplings. The most relevant measurements performed were the amplitudes of the second and fourth harmonics. The authors pointed out that amplitude measurements related to the rotational frequency of the rotor are not relevant for determining this type of failure. The modeling was done according to the Less (2007). For the angular misalignment, there is the equation 3, and for parallel misalignment, there is the equation 4.

$$f_{ang} = \frac{1}{2}\alpha_b r_b^2 \cdot \begin{bmatrix} 0 \\ 0 \\ 3k_a + k'(1+\cos(2\Omega t)) \\ k'\sin(2\Omega t) \end{bmatrix} \tag{3}$$

$$f_{par} = N_b \cdot k_b \cdot \delta_b \cdot \begin{bmatrix} \sin(\Omega t) \\ 1-\cos(\Omega t) \\ 0 \\ 0 \end{bmatrix} \tag{4}$$

For the case of angular misalignment in the formulation 4, the model proposes two rotors coupled to each other with an angle α_b. Due to this, the stiffness of one of the coupling bolts is modeled as $k_a + k'$ with the stiffness of the other bolts kept as k_a. In the model of parallel misalignment N_b, δ_b, k_b are the number of bolts in the coupling, the distance of misalignment, and the stiffness of the coupling. The input data for the simulation was sampled from the parameter distributions described in Table 2.

Shafts are very susceptible to fatigue crack nucleation and propagation, so it is of interest to monitor this type of failure. In GREEN (2005) it was verified that the second harmonic (2X) is affected in the presence of shaft cracking. According to AL-Shudeifat (2013) it is possible to simulate the presence of a transverse crack in a rotor-bearing-disk system. The author reports that during rotation, the crack opens on the shaft causing radial asymmetry due to the variation of the moment of inertia in time. Therefore, the stiffness matrix is formulated so as to generate a linear periodic system and thus introduce the crack effect into the model. The stiffness matrices of the cracked element are shown below in the matrices 5 and 6:

$$K_{c_r} = \frac{E}{l^3}\begin{bmatrix} 12I_{\bar{x}} & & & & & & & \\ 0 & -6lI_{\bar{y}} & & & & & & \\ 0 & -6lI_{\bar{y}} & 4l^2 & & & & sym. & \\ 6lI_{\bar{x}} & 0 & 0 & 4l^2 & & & & \\ -12lI_{\bar{x}} & 0 & 0 & -6lI_x & 12I_x & & & \\ 0 & -12I_{\bar{y}} & 6lI_{\bar{y}} & 0 & 0 & 12I_y & & \\ 0 & -12I_{\bar{y}} & 6lI_y & 0 & 0 & 6lI_{\bar{y}} & 4l^2 & \\ 6lI_{\bar{x}} & 0 & 0 & 2l^2I_{\bar{x}} & -6lI_x & 0 & 0 & 4l^2I_{\bar{x}} \end{bmatrix} \quad (5)$$

$$K_e = \frac{E}{l^3}\cdot\begin{bmatrix} 0 & & & & & & & \\ -12I_{\bar{X}\bar{Y}} & 0 & & & & & & \\ 6lI_{\bar{Y}\bar{X}} & 0 & 0 & & & & sym. & \\ 0 & -6lI_{\bar{Y}\bar{X}} & 4l^2I_{\bar{Y}\bar{X}} & 0 & & & & \\ 0 & 12I_{\bar{Y}\bar{X}} & -6lI_{\bar{Y}\bar{X}} & 0 & 0 & & & \\ 12I_{\bar{Y}\bar{X}} & 0 & 0 & 6l^2I_{\bar{Y}\bar{X}} & -12lI_{\bar{Y}\bar{X}} & 0 & & \\ 6lI_{\bar{Y}\bar{X}} & 0 & 0 & 2l^2I_{\bar{Y}\bar{X}} & -6lI_{\bar{X}\bar{Y}} & 0 & 0 & \\ 0 & -6lI_{\bar{Y}\bar{X}} & 2l^2I_{\bar{Y}\bar{X}} & 0 & 0 & 6lI_{\bar{Y}\bar{X}} & 4l^2I_{\bar{Y}\bar{X}} & 0 \end{bmatrix} \quad (6)$$

Where, $I_{\bar{x}} = -A_{ce}e^2$, $I_{\bar{y}} = I_y$ where A_{ce} is the cross-sectional area of the crack, e is the centroid at Y.The area moments of inertia with respect to X and Y are written as I_x and I_y, respectively. Finally, the element stiffness matrix should be replaced by the sum between the element's modified stiffness matrix by the crack stiffness matrix as $K = K_e + K_{c_r}$.

The parameters for generating the data set were sampled from probabilistic distribution as follows: angular velocity was modeled as a normal distribution, $\mathcal{N}$(50,3) [rad/s], the unbalance in both disks as a uniform distribution, $\mathcal{U}[1, 10] \cdot 10^{-6}$ $[kg \cdot m]$. For the angular misalignment simulation, the angle between the couplings was sampled from a uniform distribution, $\mathcal{U}[0.001, 1]$ [degree]. In the parallel misalignment case, the parallel distance was collected from a uniform distribution, $\mathcal{U}[1, 10]$ [mm]. Finally, for the crack shaft simulation, the crack size and the crack location were modeled from uniform distributions, $\mathcal{U}[0.01, 0.4]$ [% of radius] and $\mathcal{U}[4, 14]U[32, 42]$ [Node].

3.4 Data Generation and Processing (Full Spectrum Features)

The parameters for generating the data set were sampled from probabilistic distribution in order to create the most uniform data possible. All the parameters were modeled from uniform distributions with the exception of the angular velocity considered as a normal distribution due to its characteristic of a field measurement. In Table 2 the complete data is showed.

Table 2. Inputs Sampling Parameters for Simulation

Data Sampling for the Simulations												
For all the Fault Simualtions			**Angular Misalignment Fault**			**Parallel Misalignment Fault**			**Crack Shaft Fault**		
Parameter	**Distributions**	**Units**	**Parameter**	**Distributions**	**Units**	**Parameter**	**Distributions**	**Units**	**Parameter**	**Distributions**	**Units**
Angular Velocity	$\mathcal{N}$(50,3)	[rad/s]	Misalignment Angle	$\mathcal{U}$[0.001, 1]	[Degree]	Misalignment Distance	$\mathcal{U}$[1, 10]	[mm]	Crack Size	$\mathcal{U}$[1%, 40%]	[% radius]
Unbalance	$\mathcal{U}$[1, 10] $\cdot 10^{-6}$	[kg.m]							Crack Location	$\mathcal{U}$[4, 14] U $\mathcal{U}$[32, 42]	[Node]

The measurements used for the diagnosis with the Full Spectrum preprocessing come from the time series of the X and Y displacements of the four bearings in a time window of 0.5 seconds of the rotor system in a steady state regime. From this data processing is done by applying a Frequency analysis with a Fourier transform in x and y to obtain values of the amplitudes of the $\pm 1X$, $\pm 2X$, $\pm 3X$, $\pm 4X$, $\pm 5X$ and $\pm 6X$ harmonics, where the positive ones are related to forward and the negatives to backward. This number of harmonics used in the regression has been proved beneficial to the accuracy of the models in Belli (2023) and Belli and de Castro (2023), but in this work, the comprehension of the real need of the data will be revealed through the Sobol Index analysis.

3.5 Bayesian Neural Networks applying Monte Carlo Dropout

The dropout procedure was formalized by Srivastava *et al.* (2014) as a regularization method for neural networks, and consists of modeling the probability of a neuron participating or not in the model by a Bernoulli distribution. By applying the Monte Carlo test to the neural networks multiple predictions are obtained on the neural network with dropout. According to Gal and Ghahramani (2015) optimization based on stochastic gradient descent combined with the application of dropout during training produces the occurrence of the deep Gaussian process described by Damianou and Lawrence (2013) responsible for approximating Bayesian inference in the model. To determine the uncertainty related to prediction, multiple predictions are sampled from a neural network with dropout, and the uncertainty can be determined by calculating the standard deviation, the entropy, and the negative log-likelihood.

In rotating machinery this technique has been applied to the detection of wear levels in bearings Belli *et al.* (2022), in multi-fault rotors Belli (2023) and in the regression of rotor failure parameters Belli and de Castro (2023).

3.6 Sobol Index Analysis

The Sobol index is a sensitivity global analysis method that is used to determine the most influential inputs in the variance of the model Sobol (1990). The formulation of the first and second-order Sobol index is given by:

The total variance is given by:

$$Var(Y) = \sum_{n} Var(\mathcal{M}(X_n)) \tag{7}$$

first-order Sobol index,

$$S_n = \frac{Var(\mathcal{M}(X_n))}{Var(Y)} \tag{8}$$

where Y is the BNN output stochastic vector, the X_n is the know stochastic vector given as input variable to the model $\mathcal{M}$, and Var is the variance.

second-order Sobol index,

$$S_{n,j} = \frac{Var(\mathcal{M}(X_n, X_j))}{Var(Y)} \tag{9}$$

where X_j is the combined variable analyzed with X_i.

It's important to point out that the first-order Sobol index represents the variance effect of the input variable alone. In calculus, the focus variable is modeled as a probabilistic density function defined in finite support, the other variables remain deterministic. The analysis is performed considering just the variance of one input variable.

The second-order Sobol index considers two combined variables to analyze the combined effect. In this study, the analysis was done just to the second-order index because of the limited computational effort. Lastly, was consider a threshold of 5 % of influence in the variance to show and comment on the results section.

3.7 Analysis of the inputs

First, the BNNs are trained to regress the proposal malfunction parameters with all the available data. Then, the verification of the inverse relationship between uncertainty and accuracy is verified. The first and second-order Sobol indexes are calculated for the BNNs. Then the variables with less than 5% of importance in the variance are removed a new model is trained to verify the Sobol index relevance.

With the variable that performed less than 5% of importance on the variance in the BNNs new models are trained. It is important to notice that due to the optimation process and the fact that the models are data-driven inputs with relevant physical information can be ignored due to local minimum regions during optimization or the presence of redundant information.

During the Sobol indexes calculus the support for all the variables was determined between $[0, 1]$, this assumption is related to the normalization during the BNN training.

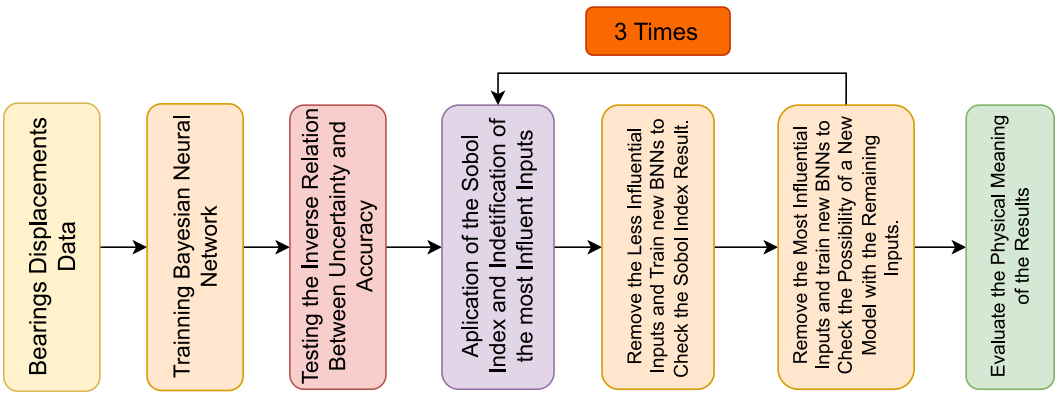

Figure 2. Methodology's Diagram.

The optimization of the hyperparameters was done using Optuna software, which is based on a Bayesian optimization algorithm of type tree-structured parzen estimator Akiba *et al.* (2019). This optimization was performed describing support of [0, 100] for the number of neurons, [0, 10] for the number of layers, and the activation functions linear, reLu, sigmoid, tangent hyperbolic, and swish. The Sobol calculus was performed using the Python library SALib Herman and Usher (2017).

4. RESULTS and DISCUSSION

Results and Discussion

Once the signal processing techniques and the conditions for preparing the training data in the model were well defined, the neural networks were trained and their architecture was optimized in a common setup for all models. Table 3 shows the common characteristics of the models. In addition, Table 4 shows the errors obtained for each model in the Mean Absolute Percentage Error (MAPE) unit.

Table 3. Bayesian Neural Network for Fault Parameter Regression

Bayesian Neural Network for Fault Parameter Regression							
Parameter	**Value**	**Parameter**	**Value**	**Parameter**	**Value**	**Parameter**	**Value**
N°. of Inputs	48	Data Collection	Bearings Displacements	Data Treatment	Full Spectrum	N°. of Neurons	63/66/70
N°. of Hidden Layers	2	N° of Outputs	1	Bias	True	Activation Function	Hyperbolic Tangent
Act. Func. (Output)	Linear	Loss Function	Mean Absolute % Error	Optimizer	ADAM	N° of Epochs	2000
Learning Rate	10^{-3}	Batch Size	10	Dropout	50%	Init. Weights Type	Random Uniform
Data Amount for Training	7500	Data Amount for Test	2500	Normalization Type	(0, 1) and log10		

Table 4. Error of Failure Parameter Regression for each Model Trained

Error of Failure Parameter Regression Models	
Model	**MAPE (Error)**
Regression of Misalignment Angle	20.8%Tr./24%Val.
Regression of Misalignment Distance	9.7%Tr./7.9%Val.
Regression of Crack Size	15.6%Tr./15.7%Val.

Below are shown partial results of the regressions performed with their uncertainty indicated by the purple shaded area.

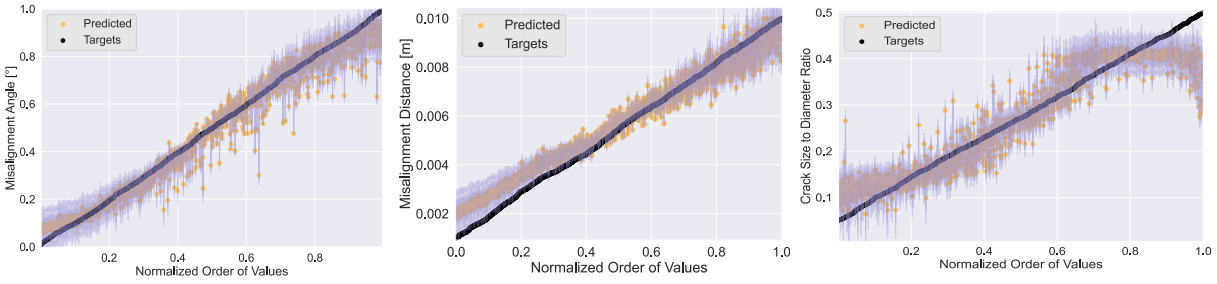

Figure 3. a) Regression of Angular Misalignment b) Regression of Parallel Misalignment Distance c) Regression of the Crack Size.

In all three fault severity regression graphs it was observed that the uncertainty tends to increase at the extremes of the fault severity. A probable reason is that in the region where the fault is not very severe, its influence is small on the vibrational behavior of the machine, and in the regions where the severity reaches its highest values it is due to the fact that non-linear phenomena start to interfere in the process. It is interesting to point out that the model for predicting crack size was able to estimate the size of cracks that changed position longitudinally and between the two shafts. Demonstrating great versatility and adaptability to the inherent characteristics of the mechanical system.

To study the behavior of the uncertainty coming from the models, graphs were generated that represents the increase in accumulated uncertainty by the accumulated error in the model predictions for the entire data set. All counts are performed from the ordering of the predictions by the uncertainty expressed in increasing form. It is expected that the uncertainty is directly proportional to the increase in error if this does not occur it means that the model is not able to represent its uncertainty and this occurs when there is a lack of adherence of the model to the training data. Below in Figure 4.

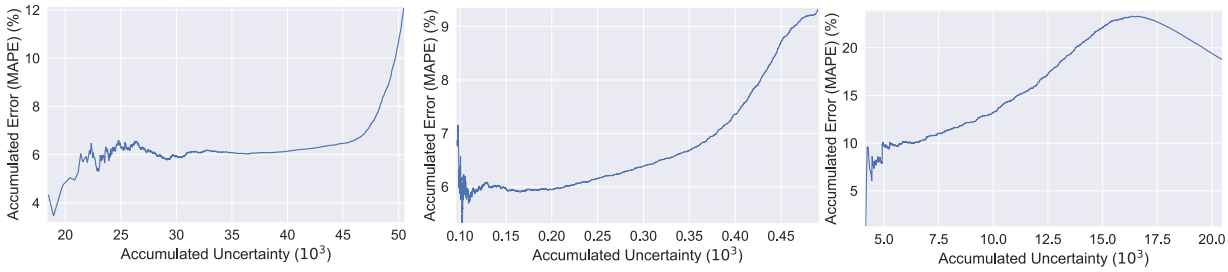

Figure 4. a) Behavior of Uncertainty in the model Regression of Angular Misalignment b) Behavior of Uncertainty in the model Regression of Parallel Misalignment Distance c) Behavior of Uncertainty in the model Regression of Crack size.

All other models showed the expected behavior trend for uncertainty and error.

4.1 Sobol Index Analysis

The Sobol index analysis was performed using the first and second-order indexes. In the majority of the cases the second-order indexes were not relevant and for this reason, were not represented integrally. The 1st order Sobol index table of the BNNs is completely demonstrated in Figure 5, 6, and 7.

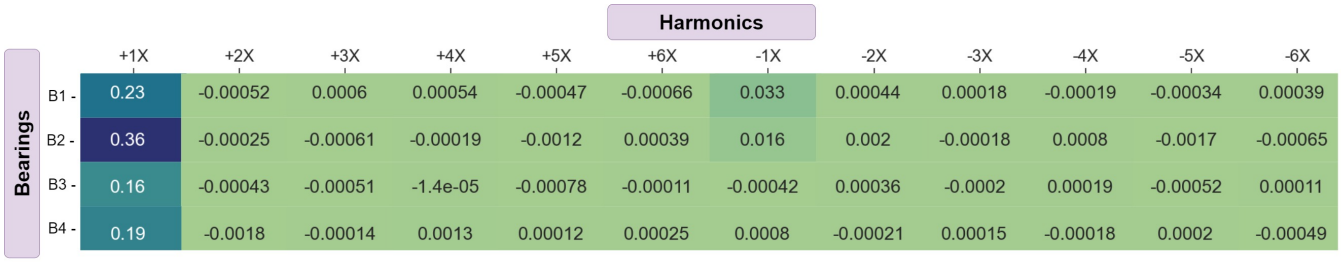

Figure 5. First Order Sobol Index Demonstration for Angular Misalignment Fault.

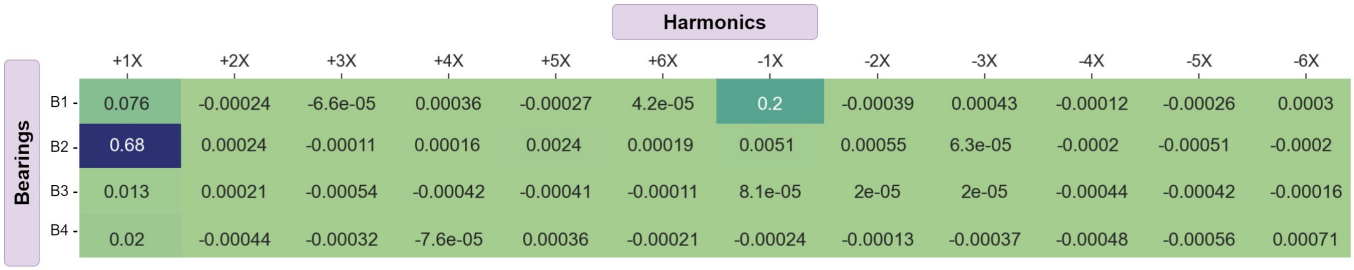

Figure 6. First Order Sobol Index Demonstration for Parallel Misalignment Fault.

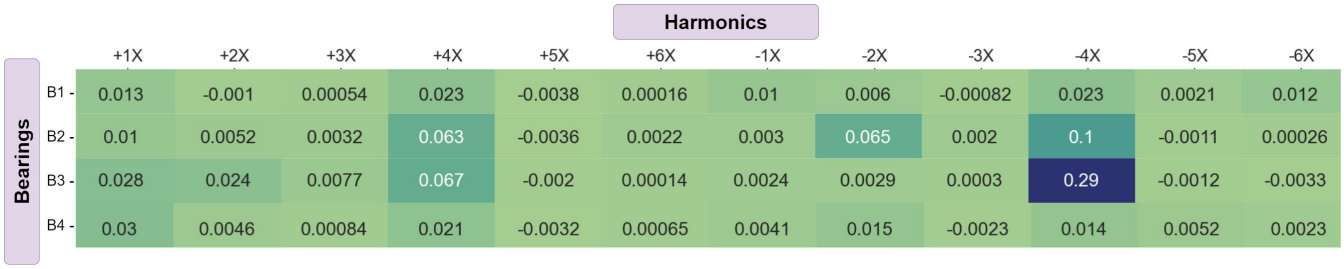

Figure 7. First Order Sobol Index Demonstration for Crack Fault.

The BNNs model for Angular Misalignment demonstrates a predominance of the first positive harmonic in the influence of the variance, with the higher index in the second bearing. Not far from that, the parallel misalignment shows a very

strong dependence of the (+1X) from the second bearing and the (-1X) from the first bearing. In the literature, the angular and the parallel misalignment are characterized by the first (+1X) and second (+2X) harmonics in qualitative diagnostics Dewell and Mitchell (1984). In the Crack size regression, the most important parameters were the (-4X) from the second and the third bearing, it is worth mentioning a discreet influence from the first (1X), fourth (4X) positive harmonics, and the second negative harmonic (2X). This result is relevant in relation to GREEN (2005) that diagnostics cracks observing the second harmonic (2X). Regarding the crack regression model, the sum of Sobol indices is more distant from unity than the other models. This factor can be explained by the limited computational resources of the study, which were not able to calculate indices of order greater than 2. It is important to emphasize that no significance was found in order-2 indices, which is why they are suppressed in this paper.

With the complete demonstration of the results of the first-order Sobol index, we notice a large number of variables with little influence in the models, and issues such as the sub-utilization of the input data gain a lot of relevance in the face of these results. In this sense, the methodology presented was applied, and the analysis and validation of the Sobol index recursively in three rounds to evaluate the potential of the data to formulate new models in the absence of other data. The results are showed in Table 5 and 6.

Table 5. Bayesian Neural Network Hyperparameters

Bayesian Neural Network Hyperparameters					
BNNs Models	**Hyperparameters**	**Round 0**	**Round 1**	**Round 2**	**Round 3**
Misalignment Angle Regression	**N° of Neurons**	63	15	86	97
	N° of Layers	1	2	4	2
	Activation	Swish	Swish	Swish	Swish
Misalignment Distance Regression	**N° of Neurons**	66	67	53	58
	N° of Layers	1	3	3	9
	Activation	Swish	Swish	Swish	Swish
Crack Size Regression	**N° of Neurons**	70	57	84	84
	N° of Layers	1	1	9	9
	Activation	Swish	Swish	Swish	Swish

Table 6. Table of Malfunction Parameter Regression Error (%) and Sobol Index

Malfunction Parameter Regression Error (%) and Sobol Index				
Sobol Index Analysis (Round 0)				
Model	**Most Relevant Inputs (1st Order Sobol Ind>5%)**	**Max 2nd Order Sobol Index**	**MAPE (Error)**	**Sobol Ind. Val. MAPE (Error)**
Misalignment Angle Regression	(+1X B1) (+1X B2)(+1X B3)(+1X B4)	0.4%	20.8%Tr./24%Val.	27%Tr./30%Val
Misalignment Distance Regression	(+1X B1) (-1X B1) (+1X B2)	0.2%	9.7%Tr./7.9%Val.	15%Tr./17%Val
Crack Size Regression	(+4X B2)(-2X B2)(-4X B2)(+4X B3)(-4X B3)	1.8%	15.6%Tr./15.7%Val.	28%Tr./35%Val
Sobol Index Analysis (Round 1)				
Model	**Most Relevant Inputs (1st Order Sobol Ind>5%)**	**Max 2nd Order Sobol Index**	**MAPE (Error)**	**Sobol Ind. Val. MAPE (Error)**
Misalignment Angle Regression	(-1X B1)(-1X B2)	11.6% ((-1X B1) + (-1X B2))	42%Tr./21%Val	31%Tr./31%Val
Misalignment Distance Regression	(+2X B2) (-1X B2) (+1X B3)(+1X B4)(-1X B4)	0.6%	17%Tr./17%Val	13%Tr./14%Val
Crack Size Regression	(+1X B1) (+4X B1) (+6X B1) (-4X B1)(+1X B2) (+2X B2)(+3X B2) (-3X B2)(+1X B3)(+2X B3)(+3X B3) (-2X B3)(+1X B4)(+4X B4)(-1X B4)(-2X B4)(-4X B4)	1.6%	17%Tr./20%Val	20%Tr./19%Val
Sobol Index Analysis (Round 2)				
Model	**Most Relevant Inputs (1st Order Sobol Ind>5%)**	**Max 2nd Order Sobol Index**	**MAPE (Error)**	**Sobol Ind, Val. MAPE (Error)**
Misalignment Angle Regression	(+2X B1)(-2X B1)(-3X B1)(+4X B2)(+5X B2) (-2X B2)(-3X B2) (-4X B2) (+2X B3)(+5X M3)(+6X B3) (-1X B3) (+2X B4)(+6X B4)(-1X B4)	1.6%	26%Tr./26%Val	37%Tr./51%Val
Misalignment Distance Regression	(+2X B1)(+3X B1)(-2X B1)(+3X B2) (+4X B2)(-2X B2)(+2X B3)(+3X B3)	1.3%	26%Tr./31%Val	24%Tr./25%Val
Crack Size Regression	(+2X B1)(+5X B1)(-1X B1)(-2X B1)(-5X B1)(-6X B1) (+6X B2)(-1X B2)(-5X B2)(+5X B3)(+2X B4)(-6X B4)	3.5%	21%Tr./21%Val	27%Tr./32%Val
Sobol Index Analysis (Round 3)				
Model	**Most Relevant Inputs (1st Order Sobol Ind>5%)**	**Max 2nd Order Sobol Index**	**MAPE (Error)**	**Sobol Ind. Val. MAPE (Error)**
Misalignment Angle Regression	(+3X B1)(+5X B2)(-6X B2)(-3X B3) (-5X B3)(-6X B3)(+6X B4)(-5X B4)	3.0%	42%Tr./40%Val	31%Tr./24%Val
Misalignment Distance Regression	(+4X B1)(+5X B1)(+6X B1)(-3X B1)(-4X B1)(-5X B1) (-6X B1)(+5X B2)(+6X B2)(-3X B2) (-4X B2) (-5X B2) (-6X B2) (+4X B3) (+6X B3) (-2X B3) (-3X B3) (-4X B3) (-5X B3) (-6X B3) (+3X B4)(+4X B4)(-2X B4) (-3X B4)(-4X B4)(-5X B4)	15.6 % ((-3X B3) + (-3X B3))	57%Tr./67%Val	27%Tr./22%Val
Crack Size Regression	(+3X B1) (+4X B1) (+6X B1) (-5X B1)(+3X B2) (-5X B2)(+3X B3)(+4X B3)(+3X B4)(-2X B4)	6.1% ((-3X B3) + (-6X B3))	31%Tr./43%Val	42%Tr./32%Val

The most important results of the table are in the last column because they refer to the validation of the Sobol indices. These accuracies were obtained by training new BNNs only with variables with Sobol index >5% in the round. In some situations, these models outperformed BNNs trained on the complete dataset of their current round. Another issue is the decrease in the accuracy of the BNNs as the rounds go by, even though there is a fluctuation in the accuracy value due to stochastic optimization, it is evident that the missing of some inputs were decisive to decrease in the accuracy of the

models.

It is interesting to note that as the rounds of Sobol Index analysis and validation progress, the number of relevant variables increases for all models. The models that showed considerable relevance in the second-order Sobol Index were the BNN for angular misalignment (round 1), parallel misalignment (round 3), and crack size (round 3) in the first round of analysis and validation.

5. CONCLUSION

The Bayesian neural networks were successful in the task of regressing the proposed failure parameters. The inverse relationship between accuracy and error was observed in all models and the global sensitivity analysis of the Sobol index was performed revealing a good coherence with other literature evidence. It is worth noting that after analyzing the BNN models trained with the full data, another analysis using the Sobol index was performed recursively in three steps. This process allowed an understanding of the sub-utilization of inputs in the model. At each round of analysis variables with Sobol index >5% were removed and new BNNs were trained on the remaining data. The second-order Sobol index was not relevant in the majority of the cases, with few exceptions in round 1 and 3. The model that performed worst in terms of accuracy obtained a MAPE error of 42% for the crack regression (In Sobol Index validation models). The proposed methodology was efficient in the sense of uniting the capacity of understanding the regression mechanism that the Sobol index provides with the quantification of uncertainty correlated to the MAPE of BNNs. In future works, this procedure could be use to select the best inputs for the model, avoiding an excessive amount of unnecessary and redundant data that are ignored by the BNN. Finally, we consider that this work was successful in demonstrating the possibility of applying artificial intelligence in environments that require high-reliability rates, helping the user to understand the predictive mechanism of the model (Sobol Index) and the regions in which the probability of the model's prediction failure is higher (BNNs Uncertainty).

6. ACKNOWLEDGEMENTS

The authors would like to thank the financial support given by the Brazilian Coordination for the Improvement of Higher Education Personnel (CAPES - grant number 88887.678075/2022-00) and National Council for Scientific and Technological Development, Brazil (CNPq - grant number 306150/2021-2).

7. AUTHORSHIP STATEMENT

The authors hereby confirm that they are the sole liable persons responsible for the authorship of this work, and that all material that has been herein included as part of the present paper is either the property (and authorship) of the authors.

8. REFERENCES

Akiba, T., Sano, S., Yanase, T., Ohta, T. and Koyama, M., 2019. "Optuna: A next-generation hyperparameter optimization framework". In *Proceedings of the 25th ACM SIGKDD International Conference on Knowledge Discovery and Data Mining*.

AL-Shudeifat, M.A., 2013. "On the finite element modeling of the asymmetric cracked rotor". *Journal of Sound and Vibration*, Vol. 332, No. 11, pp. 2795–2807. ISSN 0022-460X. doi:https://doi.org/10.1016/j.jsv.2012.12.026. URL `https://www.sciencedirect.com/science/article/pii/S0022460X12009935`.

Bae, J., Park, J.W. and Lee, S.J., 2022. "Limit surface/states searching algorithm with a deep neural network and monte carlo dropout for nuclear power plant safety assessment". *Applied Soft Computing*, Vol. 124, p. 109007. ISSN 1568-4946. doi:https://doi.org/10.1016/j.asoc.2022.109007. URL `https://www.sciencedirect.com/science/article/pii/S1568494622003271`.

Belli, O., 2023. "Development of a package for the diagnosis of rotating machines from mechanical vibrations and bayesian analysis". URL `https://hdl.handle.net/20.500.12733/9639`.

Belli, O. and de Castro, H.F., 2023. "Malfunction parameters determination using bayesian neural networks applied to a multi-fault rotor". In *Proceedings of XIX International Symposium on Dynamic Problems of Mechanics*.

Belli, O., de Moraes, M., Dias, J.P. and de Castro, H.F., 2022. "Comparison between monte carlo dropout and variational inference techniques for bayesian neural network models applied to rotating machinery diagnostics." In *Proceedings of the XLIII Ibero-Latin-American Congress on Computational Methods in Engineering*.

Castelvecchi, D., 2016. "Can we open the black box of ai?" *Nature News*, Vol. 538, No. 7623, p. 20.

Damianou, A. and Lawrence, N.D., 2013. "Deep Gaussian processes". In C.M. Carvalho and P. Ravikumar, eds., *Proceedings of the Sixteenth International Conference on Artificial Intelligence and Statistics*. PMLR, Scottsdale, Arizona, USA, Vol. 31 of *Proceedings of Machine Learning Research*, pp. 207–215. URL

https://proceedings.mlr.press/v31/damianou13a.html.

Dewell, D.L. and Mitchell, L.D., 1984. "Detection of misaligned disk coupling using spectrum analysis". *Journal of Engineering for Gas Turbines and Power*, Vol. vol.106.

Ellis, B., Heyns, P.S. and Schmidt, S., 2022. "A hybrid framework for remaining useful life estimation of turbomachine rotor blades". *Mechanical Systems and Signal Processing*, Vol. 170, p. 108805.

Fel, T., Cadène, R., Chalvidal, M., Cord, M., Vigouroux, D. and Serre, T., 2021. "Look at the variance! efficient black-box explanations with sobol-based sensitivity analysis". *Advances in Neural Information Processing Systems*, Vol. 34, pp. 26005–26014.

Friswell, M.I., 2010. *Dynamics of Rotating Machines*. Cambridge University Press.

Gal, Y. and Ghahramani, Z., 2015. "Dropout as a bayesian approximation: Representing model uncertainty in deep learning". doi:10.48550/ARXIV.1506.02142. URL https://arxiv.org/abs/1506.02142.

Garoli, G.Y., Visnadi, L.B. and de Castro, H.F., 2019. "Validation of the generalized polynomial chaos expansion to approximate the stochastic frequency response of a multi-fault rotor". *SIRM– 13th International Conference on Dynamics of Rotating Machines*.

Goodman, B. and Flaxman, S., 2017. "European union regulations on algorithmic decision-making and a "right to explanation"". *AI magazine*, Vol. 38, No. 3, pp. 50–57.

GREEN, I., C.C., 2005. "Crack detection in a rotor dynamic system by vibration monitoring - part 01: Analysis". *Journal of Engineering for Gas Turbines and Power*, Vol. vol.127. doi: 10.1115/1.1789514. URL http://gasturbinespower.asmedigitalcollection.asme.org/ on 12/18/2013 Terms of Use: http://asme.org/terms.

Hatch, C.T., 2002. *Fundamentals of Rotating Machinery Diagnostics*. Bently Nevada Press, 1st edition.

Herman, J. and Usher, W., 2017. "SALib: An open-source python library for sensitivity analysis". *The Journal of Open Source Software*, Vol. 2, No. 9. doi:10.21105/joss.00097. URL https://doi.org/10.21105/joss.00097.

Jardine, A.K., Lin, D. and Banjevic, D., 2006. "A review on machinery diagnostics and prognostics implementing condition-based maintenance". *Mechanical Systems and Signal Processing*, Vol. 20, No. 7, pp. 1483–1510. ISSN 0888-3270. doi:https://doi.org/10.1016/j.ymssp.2005.09.012. URL https://www.sciencedirect.com/science/article/pii/S0888327005001512.

Ju, L., Wang, X., Wang, L., Mahapatra, D., Zhao, X., Zhou, Q., Liu, T. and Ge, Z., 2022. "Improving medical images classification with label noise using dual-uncertainty estimation". *IEEE Transactions on Medical Imaging*, Vol. 41, No. 6, pp. 1533–1546. doi:10.1109/TMI.2022.3141425.

Krämer, E., 1993. *Dynamics of Rotors and Foundations*. Springer - Verlag, 1st edition.

Lalanne, M. and Ferraris, G., 1998. *Rotordynamics prediction in engineering*. Wiley.

Lee, H.H. and Kim, H., 2022. "Bayesian deep learning–based 1h-mrs of the brain: Metabolite quantification with uncertainty estimation using monte carlo dropout". *Magnetic Resonance in Medicine*, Vol. 88, No. 1, pp. 38–52. doi: https://doi.org/10.1002/mrm.29214. URL https://onlinelibrary.wiley.com/doi/abs/10.1002/mrm.29214.

Less, A.W., 2007. "Misalignment in rigidly coupled rotors". *Journal of Sound and Vibration*, p. 261–271.

Lund, J.W. and Sternlicht, B., 1962. "Rotor-Bearing Dynamics With Emphasis on Attenuation". *Journal of Basic Engineering*, Vol. 84, No. 4, pp. 491–498. ISSN 0021-9223. doi:10.1115/1.3658688. URL https://doi.org/10.1115/1.3658688.

Luu, D.D. and Hai, L.M., 2020. "Multi-variable regressive models for diagnostics of the unbalances on rapid rotor in shop dynamic balance". In *International Conference on Material, Machines and Methods for Sustainable Development*. Springer, pp. 267–272.

Mohanty, R.A., 1989. *Machinery Condition Monitoring: Principles and Practices*. CRC Press.

Ocvirk, F.W., 1952. "Short-bearing approximation for full journal bearings". Technical report.

Oh, D.W., Kong, S.M., Kim, S.B. and Lee, Y.J., 2023. "Prediction and analysis of axial stress of piles for piled raft due to adjacent tunneling using explainable ai". *Applied Sciences*, Vol. 13, No. 10, p. 6074.

Pan, L., Novák, L., Lehkỳ, D., Novák, D. and Cao, M., 2021. "Neural network ensemble-based sensitivity analysis in structural engineering: Comparison of selected methods and the influence of statistical correlation". *Computers & Structures*, Vol. 242, p. 106376.

Piotrowski, J., 1952. *Shaft alignment handbook*. CRC Press.

Rudin, C., 2019. "Stop explaining black box machine learning models for high stakes decisions and use interpretable models instead". *Nature machine intelligence*, Vol. 1, No. 5, pp. 206–215.

Russell, S., 2016. *Artificial Intelligence: A Modern Approach, eBook, Global Edition*. Pearson Education, Limited.

Sobol, I., 1990. "Sensitivity estimates for nonlinear mathematical models, mater".

Srinivas, R.S., Tiwari, R. and Babu, C.K., 2021. "Modeling, analysis, and identification of parallel and angular misalignments in a coupled rotor-bearing-active magnetic bearing system". *Journal of Dynamic Systems, Measurement, and Control*, Vol. 143, No. 1.

Srivastava, N., Hinton, G., Krizhevsky, A., Sutskever, I. and Salakhutdinov, R., 2014. "Dropout: A simple way to prevent

neural networks from overfitting". *Journal of Machine Learning Research*, Vol. 15, pp. 1929–1958.

Štrumbelj, E. and Kononenko, I., 2014. "Explaining prediction models and individual predictions with feature contributions". *Knowledge and information systems*, Vol. 41, pp. 647–665.

Tong, H., Hauth, J.M., Huan, X., Zhou, B.Y., Gauger, N.R., Morelli, M.C. and Guardone, A., 2022. "Bayesian recurrent neural networks for monitoring rotorcraft icing from aeroacoustics time-series data". In *AIAA Scitech 2022 Forum*. p. 2358.

Wang, S., Ren, Y., Xia, B., Liu, K. and Li, H., 2023. "Prediction of atmospheric pollutants in urban environment based on coupled deep learning model and sensitivity analysis". *Chemosphere*, Vol. 331, p. 138830.

Xie, X.h., Xu, L., Zhou, L. and Tan, Y., 2016. "Grnn model for fault diagnosis of unmanned helicopter rotor's unbalance". In *Proceedings of the 5th International Conference on Electrical Engineering and Automatic Control*. Springer, pp. 539–547.

Zang, T., Wen, G. and Zhang, Z., 2018. "Robust estimation of the unbalance of rotor systems based on sparsity control of the residual model". *Shock and Vibration*, Vol. 2018.

9. RESPONSIBILITY NOTICE

The following text, properly adapted to the number of authors, must be included in the last section of the paper: The author(s) is (are) solely responsible for the printed material included in this paper.